

Excited State Dynamics of Rh(II) Tetramesityl Porphyrin Monomer from Nanosecond Transient Absorption and Emission Spectroscopy

S. E. Vitols,[†] Duane A. Friesen,[‡] Darryl S. Williams,[‡] Dan Melamed, and Thomas G. Spiro*

Department of Chemistry, Princeton University, Princeton, New Jersey 08544

Received: July 17, 1995; In Final Form: September 26, 1995[⊗]

The excited states of [tetrakis(2,4,6-trimethylphenyl)porphyrinato]rhodium(II), Rh(II)TMP, have been studied using nanosecond transient absorption spectroscopy, emission spectroscopy, and electrochemistry. Rh(II)-TMP has a long-lived excited state, with a 460 nm absorption band, that decays with a time constant of 180 ± 22 ns, in benzene and 205 ± 28 ns in 1,3-difluorobenzene. No transient absorption features are seen between 600 and 700 nm, but weak phosphorescence is detected at 743 nm at 77 K. Thus, the excited state has the characteristics of a triplet (π, π^*) state, although a low lying, charge transfer state had been expected from iterative extended Huckel calculations. The phosphorescence is biphasic, and highly temperature dependent, consistent with a trip-quartet [⁴T] lowest excited state, lying not far below a trip-doublet [²T] state. Electrochemistry establishes that the Rh(II)/(I) reduction potential is more negative than -1.5 V versus SSCE while the porphyrin cation reduction potential is $+0.55$ V. These potentials place the lowest LMCT state at >2.05 V, well above the triplet states. In addition to elucidating the photophysics of a novel type of metalloporphyrin, these results have significant bearing on the feasibility of using Rh(II) porphyrins in photoinduced catalytic systems.

Introduction

The importance of electron transfer reactions in biological systems has prompted extensive research on the photophysics of these processes in simpler model systems. Intensive effort has been devoted to studying photoinduced charge separated states as a method for storing solar energy. A longstanding objective has been to understand photoinduced electron transfer well enough to design molecular systems that can convert solar energy into a chemical potential. Porphyrins have played a central role in this research and have been intensively investigated for their ability to participate in photoinduced electron transfer and related catalytic reactions.^{1,2} Metalloporphyrins are particularly attractive candidates in such schemes because the d orbital energies of the transition metals fall within the $\pi-\pi^*$ energy gap, thereby creating possible ligand to metal charge transfer (LMCT) and/or metal to ligand charge transfer (MLCT) states.³ The transiently reduced or oxidized metal site might subsequently undergo useful chemical reactions, as envisioned in an artificial reaction center.

Recently, intramolecular photoinduced electron transfer was investigated in a series of cobalt(II) porphyrins that were modified with covalently linked electron donor moieties.⁴ Both experimental evidence⁵ and theoretical calculations⁶ had indicated that the LMCT state for Co(II) porphyrins, Co(I)P^{•+}, lies below the lowest lying (π, π^*) excited state, making it accessible as a charge-separated intermediate. Co(I) porphyrins are known to be strong nucleophiles that can undergo alkylation reactions and even reduce protons in water.⁷ Since the lifetime of the Co(II) porphyrin excited state, 10–20 ps,⁵ is too short to support bimolecular processes in solution, a series of donor compounds were covalently linked to Co(II) porphyrins in hopes that the extended charge separation would increase the lifetime of the

CT state. Although the donors were shown to be capable of rapid electron transfer, they had no effect on the Co porphyrin excited state lifetimes. From these studies, it was concluded that the phototransient formed upon excitation is probably a ligand field state rather than the LMCT state, Co(I)P^{•+}. Given these findings, it seems likely that low-lying dd states quench the CT states for first-row transition metalloporphyrins. Consequently, for useful photoinduced electron transfer reactions, one should consider second- and third-row transition metalloporphyrins with larger dd splitting. For this reason, we turned our attention to Rh(II) porphyrins.

The excited states of Rh(II)TMP (TMP = tetramesitylporphyrin) were investigated because iterative extended Huckel (IEH) calculations lead to predictions of a low-lying LMCT state in Rh(II) monomeric porphyrin complexes.⁶ This prediction became testable with Wayland's synthesis of sterically hindered tetramesityl [TMP] complexes,⁸ which are prevented from forming dimers as is typical for Rh(II) porphyrins. Rh(II)-TMP is a monomeric, low-spin d⁷ complex. We have investigated the excited states of Rh(II)TMP, using nanosecond transient absorption and emission spectroscopy, and electrochemistry. The results establish that the lowest lying excited state of Rh(II)TMP is a mixed triplet (π, π^*) state. While the increased ligand field splitting of Rh(II) porphyrin monomers raises the dd state energies relative to Co(II) porphyrins, the charge transfer state, Rh(I)P^{•+}, is also raised above the lowest triplet state of Rh(II)TMP. Although this study presents new information on the excited state dynamics of a new class of metalloporphyrin monomers, it also suggests that Rh(II)TMP is not feasible for use in photoinduced catalytic reactions.

Materials and Methods

Synthesis of Rh Porphyrin Complexes. Chemicals were purchased from Aldrich Chemical Co. (Aldrich Chemical Co., Milwaukee, WI) and used as received, unless otherwise specified. Rh(III)TMP-Cl and Ru(II)TPP(CO)(MeOH) (Midcentury Chemical Co., Posen, IL) were checked for purity by TLC and then used as received. Thin layer chromatography plates were

* To whom correspondence should be addressed.

[†] Current address: CST-4 MSJ586 TA-46, Spectroscopy and Biophysics Group, Los Alamos, National Laboratory, Los Alamos, NM 87545.

[‡] Current address: Department of Chemistry, CB# 3290, Venable Hall, University of North Carolina at Chapel Hill, Chapel Hill, NC 27599-3290.

[⊗] Abstract published in *Advance ACS Abstracts*, December 1, 1995.

purchased from Analtech (Newark, DE). NMR measurements were taken on a General Electric 300-MHz or a JEOL 270-MHz spectrometer. All NMR samples were prepared in an inert atmosphere and the sample tubes were flame sealed. A Kratos MS50 RFA high-resolution mass spectrometer was utilized for mass spectroscopic measurements.

[Methyltetramesitylporphyrinato]rhodium[III], Rh [III]TMP-CH₃. [Chlorotetramesitylporphyrinato]rhodium[III] (50 mg, 53 μ mol) was dissolved in 25 mL of absolute ethanol and refluxed at 60 °C for 45 min followed by filtering through a fine glass frit to remove any remaining undissolved sample. The solution was refluxed under Ar for another 30 min. Sodium borohydride, NaBH₄ (15 mg, 0.396 mmol) was dissolved in 2 mL of 0.5 NaOH solution and all of it was added to the filtrate solution. The solution was then refluxed for another 45 min. Iodo-methane, CH₃I (0.1 mL) was added to the solution. A bright orange precipitate was formed. The precipitate was purified by two methods which gave identical results: (1) recrystallization from absolute ethanol; (2) thin-layer chromatography in a drybox using either 250 or 1000 μ m silica gel plates with pure chloroform as the eluant. Both methods gave pure samples of Rh(III)TMP-CH₃.⁸ UV-vis (C₆H₆): λ_{max} = 414 nm, 522 nm. ¹H NMR (δ in C₆D₆): 8.75 (pyrrole H, singlet), 7.20 (m-H, singlet), 7.07 (m'-H, singlet), 2.43 (p-CH₃, singlet), 2.26 (o-CH₃, singlet), 1.75 (o'-CH₃, singlet), -5.25 (axial CH₃, doublet). FAB MS: m/e = 898.

[Tetrakis(2,4,6-trimethylphenyl)porphyrinato]rhodium[II], Rh [II]TMP. [Methyltetramesitylporphyrinato]rhodium[III] (5 mg in \sim 5 mL of benzene) was irradiated for 15 min with 416 nm light which was generated by H₂ Raman shifting with a 10 Hz Q-switched Nd:YAG laser. UV-vis (C₆H₆): λ_{max} = 426 nm, 538 nm. ¹H NMR (δ in C₆D₆): 18.2 (pyrrole H, broad singlet), 8.86 (m-H, singlet), 3.55 (o-CH₃, singlet), 3.51 (o'-CH₃, singlet), 2.43 (p-CH₃, singlet), $t \approx$ 6.8 and 2.09 (toluene), 0.3 (CH₄). FAB MS: m/e = 883.

[(meso-Tetraphenylporphyrinato)(bis(pyridine))]ruthenium[II], Ru(II)TPP(Py)₂. 70 mg (0.9 μ M) of Ru(II)TPP(CO)-(MeOH) was dissolved in \sim 15 mL of freshly distilled pyridine (freeze-pump-thawed for three 1 h cycles) under an inert atmosphere of nitrogen. The sample was refluxed for 1 h and then irradiated by a low-pressure Hg lamp for 72 h. The pyridine was removed with a rotary evaporator. The brownish, purple solid was redissolved in a 1:1 mixture of methylene chloride and methanol. The methylene chloride was removed with a rotary evaporator. The precipitate formed in the remaining methanol was filtered and washed with heptane. UV-vis, FTIR, and ¹H-NMR peak positions matched literature values for Ru(II)TPP(Py)₂.⁹

Transient Absorption Spectroscopy. The third harmonic of a Q-switched 10 Hz Nd:YAG laser (Spectra-Physics) was used to excite a dye mixture of Stilbene 3, Coumarin 500, and Fluorol 555 that emits from 410 to 570 nm. The 20 ns broadband emission from this mixture served as the probe beam after it was focused into a bifurcated fiber optic cable. The cable was connected to a single, 0.32 m, f/4.8 single monochromator (Instruments SA) coupled to a dual diode array optical multichannel detector (Princeton Instruments). The fiber optic cable splits into two channels, one of which directs the probe beam into a pumped region of the sample; the other probes an unexcited part of the sample. The pump wavelength, 416 nm, was generated by Raman shifting in hydrogen gas. Temporal overlap between the pump and probe pulse was controlled electronically. Time zero was established by monitoring both pulses on an oscilloscope and overlapping them via timing

circuitry. The delay between the two pulses could be adjusted by increments of 10 ns.

Sample solutions were prepared under an inert atmosphere of nitrogen and diluted to a final concentration of \sim 1.7 μ M assuming an extinction coefficient of 300 000 cm⁻¹ M⁻¹ at the Soret band maximum.¹⁰ Spectral grade benzene and 1,3-difluorobenzene were freeze-pumped-thawed for three cycles. Solutions were placed in a 1 cm path length cuvette modified with a Teflon stopcock attached to the stem to prevent sample contamination with oxygen. Evidence of photochemical degradation was monitored by comparison of probe-only spectra taken before and after each time point as well as by comparison of bulk absorption spectra taken before and after each experiment. Spectra were calibrated using a holmium oxide filter and Hg, Kr⁺, and HeNe emission lines. The reported wavelengths are accurate to 2 nm.

Electrochemical Measurements. Reagent quality tetrabutylammonium perchlorate (Fluka) was recrystallized three times from ethanol and dried in a vacuum oven prior to use. 1,2-Difluorobenzene was either filtered through activated alumina or fractionally distilled and then stored over activated molecular sieves before use. Cyclic voltammograms were taken in a three-chambered cell with the counter, working, and reference electrodes arranged in a linear fashion, separated by glass frits. All potentials were referenced to a saturated sodium chloride/calomel electrode. Platinum wire (1 cm²) was used both as a counter and working electrode. The platinum electrodes were soaked in acid and heated on an open flame until red hot prior to each use to remove water and ensure a fresh surface. Measurements were performed with a Princeton Applied Research (Princeton, NJ) potentiostat. Each cyclic voltammogram was internally calibrated with the known redox couple of decamethylferrocene (-0.059 V vs SCE).

Emission Measurements. A Perkin-Elmer LS 50 fluorometer was used for static emission measurements and the phosphorescence excitation profile of Rh(II)TMP at 77 K. For the emission measurements, the sample was excited in the Soret region and scanned from 600 to 900 nm. For the excitation profile, the sample was scanned from 350 to 500 nm while monitoring the emission at 743 nm. The slit settings for both the excitation and emission monochromators were set at 5 nm. The sample was prepared as described in the transient absorption section except that the absorbance was adjusted to 0.4 OD at the Soret band maximum. The quantum yields were determined by using the optically dilute method¹¹ and the equation

$$\Phi_x = \Phi_r \left(\frac{A(\lambda)_x}{A(\lambda)_r} \right) \left(\frac{n_x^2}{n_r^2} \right) \left(\frac{D_x}{D_r} \right) \quad (1)$$

where Φ_x is the phosphorescence quantum yield, $A(\lambda)$ is the absorbance at the wavelength of the excitation, n is the refractive index, D is the integrated emission intensity, and the subscripts refer the solution of known (r) and unknown (x) quantum yields. The phosphorescence quantum yield standard was a solution of Os[II](bpy)₃(PF₆)₂ in acetonitrile at 77 K.¹²

For the time-resolved emission experiments, the sample was prepared as follows: 1,3-difluorobenzene was freeze-pumped-thaw degassed and vacuum transferred from CaH₂ prior to use. Approximately 25 mg of Rh(III)TMP-CH₃ was dissolved in 10 mL of 1,3-difluorobenzene in a drybox; the solution was filtered and then placed in a homemade cylindrical glass cell. The sample was again freeze-pumped-thawed for 3 cycles and then flame sealed. The solution was then irradiated at 420 nm with a Photon Technology International L-1 steady-state illumination system (consisting of a 75 W Xe arc lamp and Model 01-002

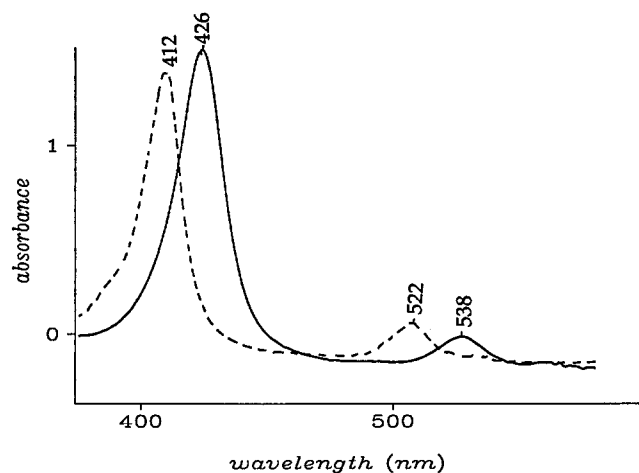


Figure 1. Ground state absorption spectra of Rh(III)TMP-CH₃ (dashed line) and Rh(II)TMP (solid line) in 1,3-difluorobenzene. The sample concentrations were 5 μ M.

grating monochromator) until the absorption spectrum had entirely converted to Rh(II)TMP (~ 15 min). The absorption spectrum was measured by a Hewlett-Packard 8451A diode-array spectrophotometer.

For the time-resolved emission measurements, Rh(II)TMP was excited with the 446 nm output of a PRA LN102 dye laser (Coumarin 450 dye), pumped by a PRA LN1000 nitrogen laser. Temperatures were maintained with a Janis 6NDT variable temperature cryostat and a Lake Shore Cryotronics DRC 84C temperature controller. The emission was detected at right angles with a PRA B204-3 monochromator/Hamamatsu R928 photomultiplier combination; stray laser light was removed with a dichromate solution filter positioned between the sample and monochromator. The signal from the PMT was recorded with a LeCroy 7200A digitizing oscilloscope which was interfaced on an IBM-PC compatible computer. The intensity vs time data were fitted to a biexponential function: $I(t) = A \exp[-(k_1 t)] + B \exp[-(k_2 t)]$. The absorption spectrum was checked after completion of the emission measurements and no changes were noted.

Results

The porphyrin Soret and Q absorption bands are red-shifted by approximately 20 nm when Rh(III)TMP-CH₃ is photolyzed to Rh(II)TMP in solution (Figure 1). Our photolysis procedure, involving 15 min exposure to 1.5 mW of 416 nm light from a 10 Hz Q-switched Nd:YAG laser, improves on the previous 6 h irradiation in a Rayonet photoreactor⁸ by reducing the preparation time. The Rh(II)TMP, generated by 416 nm light photolysis, was pure as indicated by the visible absorption and ¹H NMR spectra.

Nanosecond transient absorption difference spectra of Rh(II)TMP in benzene and 1,3-difluorobenzene (Figure 2) were obtained in the 400–600 nm region, with zero delay between the 416 nm excitation pump pulse and the probe pulse. Bleaching is seen for the ground state Soret band at 430 nm and for the Q band at 540 nm. In addition, a broad, induced absorption is seen at ~ 460 nm. Within 1 μ s, the bleach of the ground state Soret band was observed to recover and the induced transient had completely disappeared. The lifetime of the lowest-lying excited state was determined by measuring the bleach of the Soret from 0 ns to 1 μ s at 100 ns intervals. A first order kinetic fit ($R = 0.99$) of the data (Figure 3) yielded lifetimes of approximately 200 ns for Rh(II)TMP in both solvents. A similar, but much longer-lived ($> 2 \mu$ s) induced absorption was

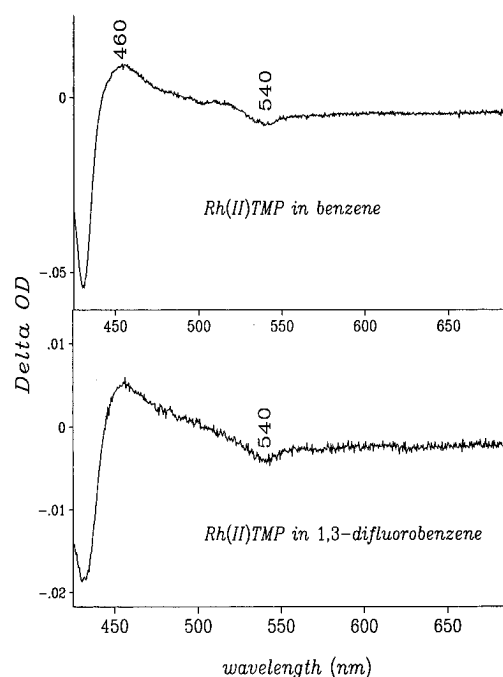


Figure 2. Transient absorption difference spectra from 400 to 650 nm with overlapped pump and probe pulses for Rh(II)TMP in benzene (top) and in 1,3-difluorobenzene (bottom). Excitation was provided by 2 mJ, 7 ns pulses at 416 nm (10 Hz).

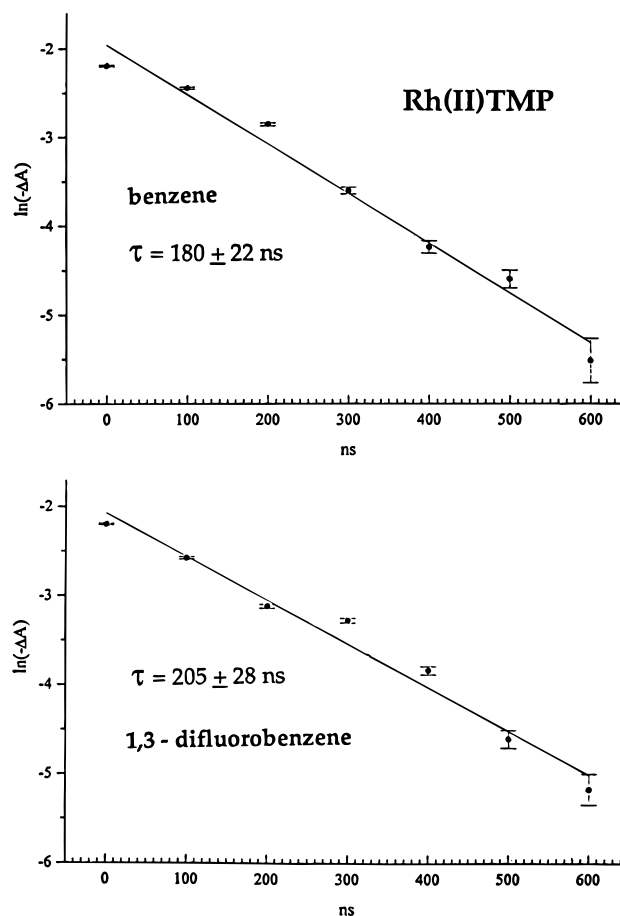


Figure 3. First order decay plots for the absorbance differences at the Soret maximum for photoexcited Rh(II)TMP in benzene (top) and 1,3-difluorobenzene (bottom). Conditions as in Figure 2, with electronically adjusted delays of 100 ns between excitation and probe pulses.

observed for Rh(III)TMP-Cl (data not shown), which is known to have a triplet $\pi-\pi^*$ state as its lowest lying excited states.¹³

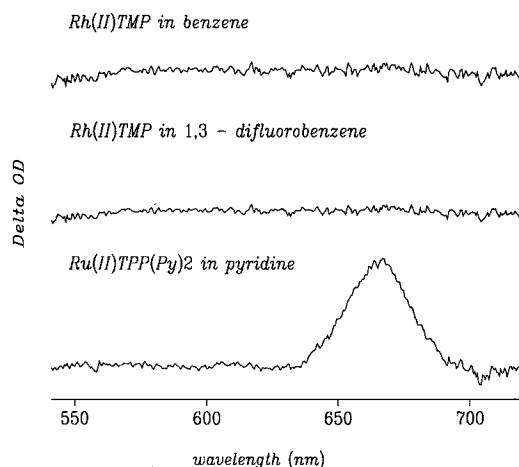


Figure 4. Transient absorption difference spectra (0 ns delay) from 550 to 700 nm for Rh(II)TMP in benzene and in 1,3-difluorobenzene (upper panel) and Ru(II)TPP(Py)₂ in pyridine (lower panel). Excitation was provided by 2 mJ, 7 ns pulse at 416 nm (10 Hz).

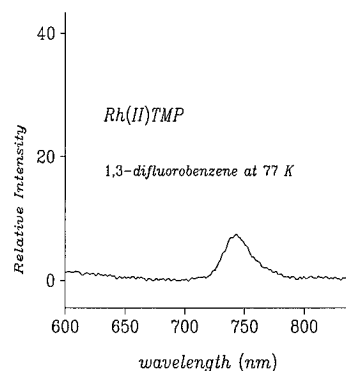


Figure 5. Luminescence spectrum for Rh(II)TMP in 1,3-difluorobenzene at 77 K. Excitation was at 425 nm.

TABLE 1: Photophysical Properties of Rh(II) Tetramesitylporphyrin Relative to Rh(III) Octaethyl- and Tetraphenylporphyrins

compound	phosphorescence (77 K)		triplet (RT) ^a τ
	T(0,0) (nm)	ϕ_p	
Rh(II)TMP	750	0.01	200 ns
Rh(III)TPP-Cl ¹⁹	718	0.07	115 μ s
Rh(III)OEP-Cl ³³	659	0.24	NM ^b
Rh(III)TPPS ₄ ³⁻³⁴	709	0.07	350 μ s

^a RT = room temperature. ^b Not measured.

One can distinguish between π - π^* triplets and charge transfer excited state by examining transient spectra between 600 and 700 nm, since the latter show induced absorptions in this region while the former do not.¹⁴ This absorption is demonstrated in Figure 4 for Ru(II)TPP(Py)₂ which is known to have a ³(d, π^*) charge transfer excited state.⁹ However, no induced absorptions are seen in this region for Rh(II)TMP, either in benzene or in 1,3-difluorobenzene.

Upon excitation at 425 nm, Rh(II)TMP gives rise to a 743 nm phosphorescence band at 77 K in 1,3-difluorobenzene (Figure 5), with a quantum yield of 0.01. No phosphorescence is observed at room temperature for Rh(II)TMP. Relative to Rh(III) porphyrins (Table 1), the phosphorescence for Rh(II)TMP occurs at lower energies (~ 1300 to 3600 cm⁻¹) and has a reduced quantum yield. The red shift of the phosphorescence is consistent with the lower energy of the Rh(II)TMP Q band (Figure 1). The phosphorescence excitation spectrum (Figure 6) of Rh(II)TMP at 77 K tracks the Soret absorption band but with a ~ 6 nm red shift. A similar red shift was observed for

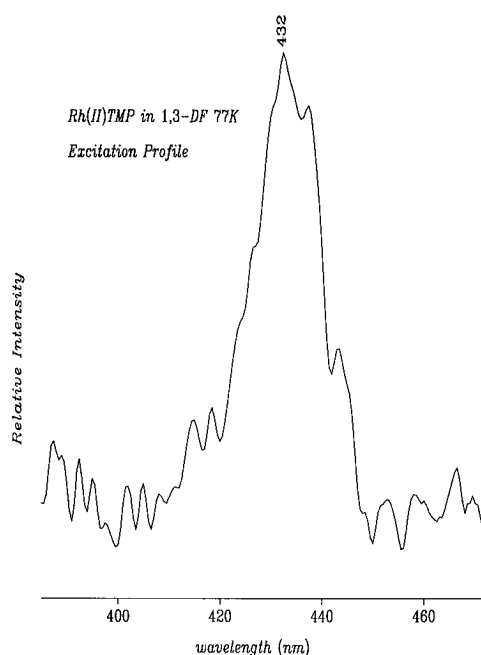


Figure 6. Phosphorescence excitation spectrum for Rh(II)TMP in 1,3-difluorobenzene at 77 K. Emission was monitored at 743 nm. The noise in the spectrum reflects the weak emission and the poor glassing properties of the solvent.

TABLE 2: Temperature Dependence of Rh(II)TMP Phosphorescence in 1,3-Difluorobenzene^a

T (K)	k ₁ (s ⁻¹)	τ_1 (μ s)	k ₂ (s ⁻¹)	τ_2 (μ s)
130	5.25E+03 ^a	191	1.71E+04	59
160	5.1E+03	195	2.21E+04	45
190	7.25E+03	138	6.92E+04	14
230	1.89E+04	53	9.72E+04	10

^a Data fitted to biexponential function $I(t) = A \exp[-(k_1 t)] + B \exp[-(k_2 t)]$. Temperature dependence data collected with $\lambda_{em} = 745$ nm. E+03 $\equiv \times 10^3$.

the Soret band of Cu(II)OEP in methylcyclohexane at 77 K.¹⁵ The excitation spectrum establishes that no species other than Rh(II)TMP contributes to the phosphorescence. Table 2 gives the results of the time-resolved emission measurements. The intensity vs time data showed two components which were fitted to successive exponential decays.

Well-resolved cyclic voltammograms were recorded for Rh(III)TMP-Cl and Rh(III)TMP-ClO₄ (Figures 7 and 8) between +1.2 and -1.5 V vs SCE. Different voltammograms are obtained by holding the potential at -1.4 V (Figure 7) or -1.0 V (Figure 8) because the chloride ligand is lost upon reduction. The first reduction process is seen as an irreversible wave, centered at approximately -0.85 V (Figure 7, top), reflecting the chloride ligand loss, but initiating the voltammogram at -1.4 V (Figure 7, bottom) causes the Rh(III)/Rh(II) couple to become reversible at -0.39 V. The reversibility of the Rh(III)/Rh(II) couple, once chloride is replaced by perchlorate ion from the supporting electrolyte, implies that no chemistry is taking place with the solvent, 1,2-difluorobenzene, during the scan. This observation is significant because other rhodium(III) porphyrin perchlorates are known to be very strong electrophiles, capable of aromatic substitution,¹⁶ a reactivity that produces irreversibility in the Rh(III)/Rh(II) couple. This reactivity is not observed for Rh(III)TMP-ClO₄ on the time scale of these voltammograms. No additional reductions were observed before reaching the solvent limit at -1.5 V. Thus, the Rh(II)/Rh(I) reduction potential is at least this negative.

Oxidation of Rh(III)TMP is also dependent on the nature of

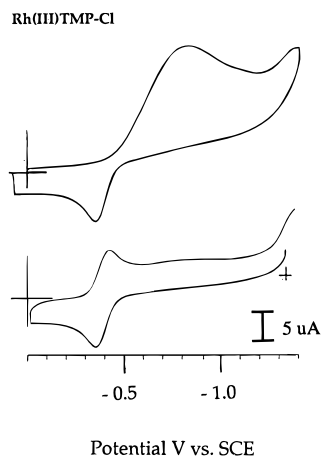


Figure 7. Cyclic voltammograms of Rh(III)TMP-Cl in 1,2-difluorobenzene with 0.1 M tetrabutylammonium perchlorate. The scan rate is 100 mV/s. (Top) The scan is initiated at 0.0 V. (Bottom) The scan is initiated at -1.45 V, shown at the smaller cross hair.

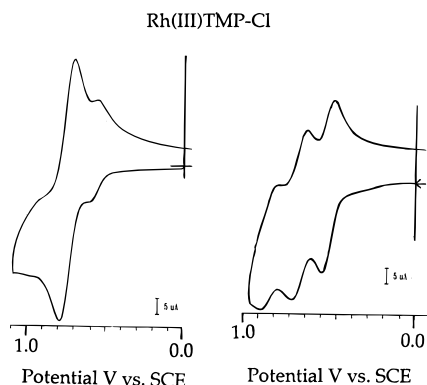


Figure 8. Cyclic voltammogram of the oxidation of Rh(III)TMP-Cl, solvents and conditions are identical to those in Figure 6. (Right) The scan is initiated at 0.0 V. (Left) The scan is initiated at -1.0 V.

its axial ligand. Two oxidation waves are seen in Figure 8, whose amplitudes depend on the initiation potential. When the potential is held initially at -1.0 V, the wave at $+0.55$ V increases at the expense of the wave at $+0.74$ V. We therefore assign the former wave to Rh(III)TMP-ClO₄ and the latter one to Rh(III)TMP-Cl. The oxidation involves removal of an electron from the porphyrin ring. Thus, the redox potential for the π radical cation formation is ~ 200 mV higher for the chloride than for the perchlorate species. This observation is consistent with trends previously reported for rhodium porphyrins.^{17–20} An additional oxidation wave is seen at $+0.95$ V (Figure 8, right panel), which is assigned to the second porphyrin oxidation in the perchlorate adduct. A complete scheme for both the oxidative and reductive redox chemistry of the rhodium tetramesityl porphyrin is shown in Figure 9.

Discussion

Based on IEH calculations, the lowest-lying excited state of Rh(II)TMP had been expected to be a LMCT state.⁶ However, the results of transient absorption, emission, and electrochemical measurements make clear that the lowest lying excited state is a mixed triplet (π, π^*) state. Between 400 and 600 nm, the transient absorption difference spectra show a broad, induced absorption with a maximum at 460 nm. This feature, occurring between the ground state Soret and Q bands, is characteristic of $^1(\pi, \pi^*)$ and $^3(\pi, \pi^*)$ states observed in many other metalloporphyrins.¹⁴ The excited state is too long lived for it to be a singlet since the lifetimes of $^1(\pi, \pi^*)$ states in metalloporphyrins

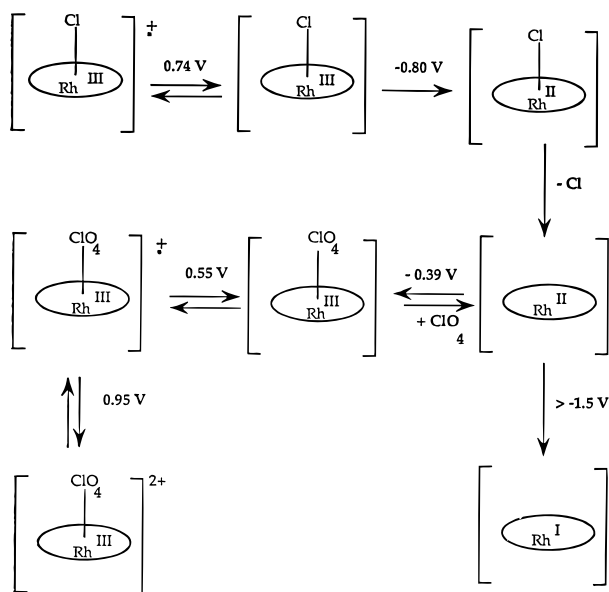


Figure 9. Proposed scheme for the redox chemistry of Rh(III)TMP-Cl in 1,2-difluorobenzene with TBAClO₄ as supporting electrolyte.

rins range from 700 ps to 12 ns.¹⁴ Moreover, $^1(\pi, \pi^*)$ spectra show a characteristic Q(0,1) stimulated emission band which manifests itself as a negative feature embedded in the background absorption to the red of the Q band bleach.¹⁴ No such feature is seen in the transient absorption difference spectra of Rh(II)TMP. Furthermore, Rh(II)TMP exhibits emission in the far red that is characteristic of triplet phosphorescence.

The transient difference spectra obtained between 600 and 700 nm also argue against the lowest lying excited state being charge transfer in character. No induced features are seen for Rh(II)TMP in this region, in contrast to Ru(II)TPP(Py)₂ which shows a pronounced MLCT absorption at 670 nm. The absence of an induced absorption in this region further supports the assignment of the induced absorption observed in the blue for Rh(II)TMP as being (π, π^*) in character.

Finally, an LMCT state involves charge separation and its lifetime should depend on solvent polarity because the rate of back electron transfer contains a free energy term, ΔG° , that is connected through λ , the reorganizational energy, to the dielectric constant of the solvent.^{21,22} However, the lifetime of the lowest lying excited state of Rh(II)TMP is ~ 200 ns in both benzene and 1,3-difluorobenzene even though the static dielectric constant, ϵ_0 , for 1,3-difluorobenzene is 10 times larger than that of benzene.

The electrochemical measurements reveal the reason for the excited state being (π, π^*) rather than LMCT in character: Rh(II)TMP is difficult to reduce to Rh(I). In fact, the Rh(II)/Rh(I) reduction could not be directly observed because it is beyond the solvent limit of 1,2-difluorobenzene. Other solvents with more negative limits were excluded by the reactivity of Rh(II)TMP which reacts with sp^3 hybridized carbon bonds. Using -1.5 V as the lower limit for the Rh(II)/Rh(I) reduction potential, one can use the Suppan relationship to calculate the exothermicity, ΔU_{cs} , of a photoinduced electron transfer:²³

$$-\Delta U_{cs} = E_{S1} - E_D^{\text{ox}} + E_A^{\text{red}} \quad (2)$$

where E_{S1} is the energy of the lowest singlet state (estimated from the Q band maximum at 2.31 eV), E_D^{ox} is the oxidation potential for the porphyrin (0.55 V) and E_A^{red} is the (Rh[II]/Rh[I]) reduction potential (> -1.5 V). These numbers give a $-\Delta U_{cs}$ value $< +0.32$ eV. Consequently, the LMCT state must

be >2.05 eV, well above the triplet state, which is estimated from the phosphorescence maximum to be at 1.65 eV.

Since Rh(II) reduction places an electron in the d_z^2 orbital, the d_z^2 orbital energy must be >1.5 eV. By contrast, the IEH calculations place the d_z^2 orbital at much lower energies.⁶ Consistent with the higher energy estimate from electrochemistry is the recent work of Wayland and co-workers who carried out EPR studies on a series of Rh(II)TMP-X complexes with a series of σ donor or π acceptor ligand.²⁴ The energy gap between the d_z^2 and (d_{xz} , d_{yz}) orbitals, $\Delta E_{xz, yz \rightarrow d_z^2}$ was found to range from 1.73 to 2.50 eV (14 000 to 20 000 cm^{-1}).²⁴ The IEH calculations, on the other hand, predict $\Delta E_{xz, yz \rightarrow d_z^2}$ to be on the order of ~ 0.2 eV.⁶ The experimental results, from both this work and the EPR measurements, indicate that splitting between the d orbitals of Rh(II) monomeric porphyrins is much larger than calculated.

These results underscore the unreliability of using IEH calculations as a guide for finding and investigating CT states in metalloporphyrins. As previously noted by Gouterman,²⁵ the IEH method does not accurately predict the transition energies for charge transfer states. In the case of Zn(II) porphyrin complexes, IEH calculations predicted a low-lying b_{1g} ($\text{Np}\sigma$, $d_{x^2-y^2} \rightarrow e_g(\pi^*)$) transitions.²⁵ For the Zn(II) complexes, the existence of strong emission for the (π, π^*) states contradicts this prediction and indicates that this CT transition occurs at much higher energies. So, while the IEH method has proven to be a reliable tool in mapping out and understanding the terrain of the principal (π, π^*) transitions in metalloporphyrins, it should not be used as a guide for finding and investigating CT states.

The triplet lifetime for Rh(II)TMP, 200 ns at room temperature, is unusually short; Rh(III) porphyrin triplet states, for example, live for several hundred microseconds.¹⁵ We attribute the faster decay to deactivation through a tripdoublet state. Rh(II) porphyrins have d^7 electronic configurations and the unpaired d electron interacts with the singlet and triplet states of the porphyrin to generate doublets, $^2S_0(\pi, \pi^*)$ and $^2T(\pi, \pi^*)$ as well as quartets, $^4T(\pi, \pi^*)$. The magnitude of the interaction is modest, however, and the doublet/quartet splittings are not large; 200–700 cm^{-1} gaps have been estimated for Cu(II) porphyrins, which also have tripdoublet and quartet states due to their d^9 electronic configurations.^{15,26–28} Consequently, the higher lying tripdoublet state may be thermally accessible, and can provide efficient deactivation, since it has the same spin multiplicity as the ground state 2S_0 . This interpretation is supported by the low-temperature, time-resolved emission measurements which show two exponential decays, each rate slowing down as the temperature is lowered. The shorter lifetime, 10 μs at 230 K, is attributable to direct emission from the 2T state; it lengthens continuously with decreasing temperature, reaching 60 μs at 130 K. The longer lifetime is attributable to the 4T state; it increases dramatically (by a factor of nearly 3) between 230 and 190 K and then levels off at ~ 200 μs below 160 K.

Figure 10 illustrates the relative ordering of the energy states for Rh(II)TMP and how rapid relaxation can occur through a doublet pathway at room temperature. In noncoordinating solvents, similar behavior has been observed in the photophysics of Cu(II)OEP,^{15,23} which has a lifetime of 10 μs at 150 K but only 270 ns at room temperature. In the case of Cu(II)OEP, the temperature dependence is attributed to a thermally accessible charge transfer state. However, given the lack of dependence on solvent polarity for the Rh(II)TMP excited state lifetimes measured at room temperature and the high redox potential estimated for the Rh(II)/(I) reduction, a nearby-charge transfer state is ruled out for Rh(II)TMP.

Although a number of polypyridyl complexes of transition

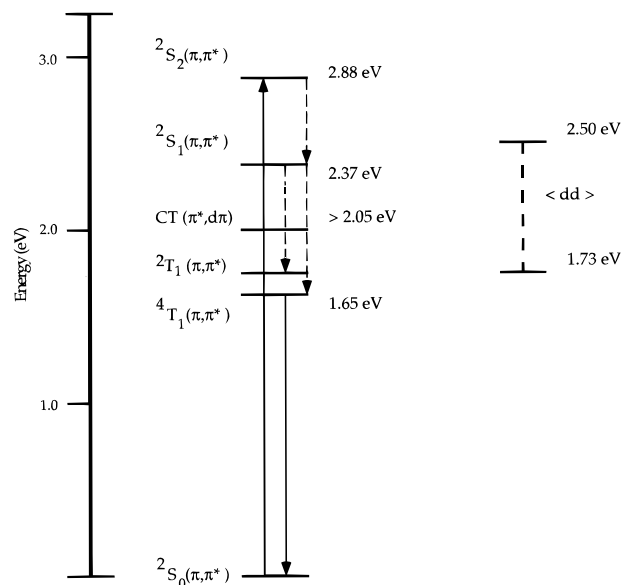


Figure 10. Schematic energy level diagram showing the low-lying excited states of Rh(II)TMP.

metals display a rich variety of photoinduced metal redox chemistry,^{29–31} it is evident that utilizing the CT photochemistry of metalloporphyrins will require careful attention to both the dd and triplet state energies. The first-row transition metalloporphyrins are poor candidates because their ligand field states lie at lower energies than the triplet states. A second-row transition metal, such as Rh(II), has larger d orbital splittings and the additional attractive feature of increased spin–orbit coupling. Increased spin–orbit coupling can generate longer-lived CT states by mixing in triplet character. The prototypical example of this is $\text{Ru}(\text{bpy})_3^{2+}$ which has a long-lived 650 ns MLCT state that contains substantial triplet character.³²

Unfortunately, in the case of Rh(II)TMP, the acceptor d orbital is raised too high in energy, so that the CT state is higher than the lowest (π, π^*) state. This state has a mixed triplet character and its intrinsic lifetime is substantially shortened by relaxation through doublet states generated via spin–orbit coupling.

One strategy for altering the energy of the LMCT state relative to the other states in Rh(II)TMP is through coordination of an axial ligand. In fact, Wayland has demonstrated the sensitivity of the d orbital energies of Rh(II) porphyrins to axial ligand coordination by generating a series of Rh(II) porphyrin adduct complexes where the adduct ligand is either a σ donating or π accepting ligand.²⁷ Low-temperature EPR studies indicate that adduct formation with π acceptor ligands generally gives greater d orbital splitting than with σ donating ligands. Unfortunately, both types of ligands raise the overall energy of the HOMO d_z^2 orbital, thereby raising the energy of the CT state.

Ruthenium porphyrins are also affected by the nature of the adduct ligand bound to the metal.³² However, unlike Rh(II)TMP, the HOMO orbitals of Ru(II) are d_{xy} , not d_z^2 . Therefore, the CT state is metal-to-ligand in character and coordination of σ donating ligands such as pyridine lowers the CT state relative to the triplet state. The MLCT state of a ruthenium porphyrin is expected to be that of a Ru(III) porphyrin radical anion. Unfortunately, Ru(III) is not a particularly reactive metal³³ and holds small hope for photoinduced redox chemistry.

However, photoexcited Ru(II) porphyrins are known to undergo efficient oxidative/reductive quenching reactions with suitable acceptor/donor molecules.^{34,35} In fact, $[\text{Ru}(\text{TTP})(\text{py})_2]^*$ is known to be a better reductant by -0.6 V than $\text{Ru}(\text{bpy})_3^{2+*}$.

Consequently, the excited state reductive properties of [Ru(TPP)(py)₂]* are exploitable in bimolecular reductive schemes similar to those developed for Ru(bpy)₃²⁺*, particularly regarding water reduction. The reduction of water to hydrogen requires -0.41 V at pH = 7; subsequently, one could envision a water-soluble analog of [Ru(TPP)(py)₂]* reducing water directly or serving as a potent photosensitizer for generating reduced methyl viologen (MV⁺), which, in turn, has sufficient redox potential for hydrogen evolution from water. Consequently, the excited state redox properties of Ru(II) porphyrins may prove more useful than those of Rh(II) porphyrins.

Acknowledgment. We thank Professors Dewey Holten and Glen Loppnow for insightful discussions. The synthetic chemistry and NMR measurements were done with the kind and generous instruction of J. Scott Roman and Dr. Robert Goodnow. Dr. Geoffrey Strousse kindly provided the sample of Os[III](bpy)₃(PF₆)₂. This work was supported by DOE grant DE-FG02-88ER13876.

References and Notes

- (1) Lehn, J.-M. *Agnew. Chem., Int. Ed. Engl.* **1988**, 27, 89.
- (2) Wasielewski, M. R. *Chem. Rev.* **1992**, 92, 435.
- (3) Gouterman, M. In *The Porphyrins, Volume III—Physical Chemistry, Part A*; Dolphin, D., Ed.; Academic Press: New York, 1978.
- (4) Loppnow, G. R.; Melamed, D.; Leheny, R. A.; Hamilton, A. D.; Spiro, T. G. *J. Phys. Chem.* **1993**, 97, 8969.
- (5) Tait, C. D.; Holten, D. *Chem. Phys. Lett.* **1983**, 105, 4896.
- (6) Antipas, A.; Gouterman, M. *J. Am. Chem. Soc.* **1983**, 105, 4896.
- (7) Kellett, R. M.; Spiro, T. G. *Inorg. Chem.* **1985**, 24, 2373.
- (8) Wayland, B. B.; Ba, S.; Sherry, A. E. *J. Am. Chem. Soc.* **1991**, 113, 5305.
- (9) Levine, L. M. A.; Holten, D. *J. Phys. Chem.* **1988**, 92, 714–720.
- (10) Smith, K. M. *Porphyrins and Metalloporphyrins*; Elsevier: New York, 1975.
- (11) Demas, J. N.; Crosby, G. A. *J. Phys. Chem.* **1971**, 75, 991–1024.
- (12) Pankuch, B. J.; Lucky, D. E.; Crosby, G. A. *J. Phys. Chem.* **1980**, 84, 2061.
- (13) Hoshino, M.; Seki, H.; Yasufuku, K.; Shizuka, H. *J. Phys. Chem.* **1986**, 90, 5149.
- (14) Rodriguez, J.; Kirmaier, C.; Holten, D. *J. Am. Chem. Soc.* **1989**, 111, 6100.
- (15) Yan, X.; Holten, D. *J. Phys. Chem.* **1988**, 92, 5982.
- (16) Aoyama, Y.; Yoshida, T.; Sakurai, K.-I.; Ogoshio, H. *Organometallics* **1986**, 5, 168–173.
- (17) Kadish, K. M. *Prog. Inorg. Chem.* **1986**, 34, 435–605.
- (18) Wayland, B. B.; Newman, A. R. *Inorg. Chem.* **1981**, 20, 3093.
- (19) Anderson, J. E.; Yao, C.-L.; Kadish, K. M. *Inorg. Chem.* **1986**, 25, 3225.
- (20) Kadish, K. M.; Hu, Y.; Boschi, T.; Tagliatesta, P. *Inorg. Chem.* **1993**, 32, 2996.
- (21) Weller, A. Z. *Phys. Chem. N. F.* **1982**, 133, 93–98.
- (22) Marcus, R. A.; Sutin, N. *Biochim. Biophys. Acta* **1985**, 811, 265–322.
- (23) Wasielewski, M. R.; Niemczyk, M. P.; Svec, W. A.; Pewitt, E. B. *J. Am. Chem. Soc.* **1985**, 107, 1080–1082.
- (24) Wayland, B. B.; Sherry, A. E.; Bunn, A. G. *J. Am. Chem. Soc.* **1993**, 115, 7675–7684.
- (25) Gouterman, M.; Hanson, L. K.; Khalil, G.-E.; Leenstra, W. R.; Buchler, J. W. *J. Phys. Chem.* **1975**, 79, 2343.
- (26) Smith, B. E.; Gouterman, M. *Chem. Phys. Lett.* **1968**, 2, 517–519.
- (27) Gouterman, M.; Mathies, R. A.; Smith, B. E. *J. Chem. Phys.* **1970**, 52, 3795.
- (28) Kim, D.; Holten, D.; Gouterman, M. *J. Am. Chem. Soc.* **1984**, 106, 2793.
- (29) Malouf, G.; Ford, P. C. *J. Am. Chem. Soc.* **1977**, 99, 7213.
- (30) DeArmond, M. K.; Myrick, M. L. *Acc. Chem. Res.* **1989**, 22, 364.
- (31) Kober, E. M.; Caspar, J. V.; Sullivan, B. P.; Meyer, T. J. *Inorg. Chem.* **1988**, 27, 4597.
- (32) Kalyanasundaram, K. *Photochemistry of Polypyridine and Porphyrin Complexes*; Academic Press: New York, 1992; p 626.
- (33) Brown, G. M.; Hopf, F. R.; Ferguson, J. A.; Meyer, T. J.; Whitten, D. G. *J. Am. Chem. Soc.* **1975**, 97, 5939–5942.
- (34) Rillema, D. P.; Nagle, J. K.; Barringer, L. F.; Meyer, T. J. *J. Am. Chem. Soc.* **1981**, 103, 56.
- (35) Young, R. C.; Nagle, J. K.; Meyer, T. J.; Whitten, D. G. *J. Am. Chem. Soc.* **1978**, 100, 4773.

JP952003H